Analyst

ROYAL SOCIETY OF CHEMISTRY

PAPER

View Article Online
View Journal

Cite this: DOI: 10.1039/d0an01469a

A two-chip acoustofluidic particle manipulation platform with a detachable and reusable surface acoustic wave device†

Jingui Qian, [a] Jifeng Ren,[b] Yi Liu,[b] Raymond H. W. Lam [b] and Joshua E.-Y. Lee *[a,c]

Received 25th July 2020,
Accepted 1st September 2020

DOI: 10.1039/d0an01469a

rsc.li/analyst

This work describes a two-chip acoustofluidic platform for two-dimensional (2D) manipulation of microparticles in a closed microchamber on a reusable surface acoustic wave (SAW) device. This platform comprises two microfabricated chips: (1) a detachable silicon superstrate enclosed by a PDMS microfluidic chamber and (2) a reusable SAW device for generating standing SAW (SSAW), which is typically an expensive component. Critical to such a two-chip acoustofluidic platform is the selection of a suitable coupling agent at the interface of the SAW device and superstrate. To this end, we applied a polymer thin film as a coupling agent that balances between acoustic coupling efficiency, stability over time, and reusability. Recycling of the SAW device lowers the cost-barrier for acoustofluidic particle manipulation. The SSAW is transmitted into the silicon superstrate *via* the coupling agent to form a standing Lamb wave (SLW) to trap and move microparticles. The reported two-chip strategy enables the single-use microfluidic superstrates to avoid chemical and biological contaminations, while maintaining the merits of acoustofluidic manipulation of being noncontact and label-free and applicable to a wide range of microparticles with different shapes, density, polarity, and electrical properties.

Introduction

Cell manipulation and separation techniques are essential for fundamental biological analyses, such as isolating circulating tumour cells (CTCs) from human blood cells.[1–5] Recently, acoustically driven fluidic manipulation techniques have received reasonable interest for being contactless, label-free, biocompatible, and pollution-free and consume much less power than optical tweezers.[6–14] Acoustic tweezers can be applied to a wide range of particles, independent of shape, density, electrical properties and polarity. Acoustic tweezers are able to control microparticles by adjusting the frequency, phase and power of the input radio frequency (RF) signal.[15] Most acoustic tweezers have traditionally been based on single-use and non-reusable surface acoustic wave (SAW) devices where the fluid interacts directly with the SAW. The price of SAW substrates, *e.g.* lithium niobate (LN), is still rather costly, which poses a significant challenge to the cost-effectiveness of single-use platforms, limiting further applicability in chemical and biological analyses, in which no contamination is permitted.[16]

More recently, different researchers have demonstrated reusable acoustofluidic platforms comprising an LN SAW substrate that drives an acoustic wave into a disposable silicon superstrate where particles in fluid are loaded. These two-chip acoustofluidic platforms have predominantly been used for centrifugation, concentration, and separation in a sessile droplet.[17] While there exist many references on two-chip acoustofluidic droplet concentration (and mostly on silicon superstrates), there are very few reports on two-chip devices for particle manipulation. One of the few and excellent examples of a two-chip device for particle manipulation is work by Guo *et al.* based on glass superstrates and using a coupling liquid.[18] In fact, a few liquids like water, UV epoxy and gel have been applied as coupling agents.[17,18] While coupling liquids generally work well for droplet concentration, the higher RF power required for particle manipulation induces technical challenges such as evaporation and degradation of the coupling liquid during operation, and requires additional clips to affix the silicon superstrate to the SAW device.

Therefore, critical to the realization of two-chip acoustofluidic manipulation platforms is identifying a suitable solid coupling agent that simultaneously addresses both issues of

[a]Department of Electrical Engineering, City University of Hong Kong, Kowloon, Hong Kong SAR. E-mail: josh.lee@cityu.edu.hk; Tel: +852 3442 9897
[b]Department of Biomedical Engineering, City University of Hong Kong, Kowloon, Hong Kong SAR
[c]State Key Laboratory of Terahertz and Millimeter Waves, City University of Hong Kong, Kowloon, Hong Kong SAR

† Electronic supplementary information (ESI) available. See DOI: 10.1039/d0an01469a

stability and detachability. In this paper, we show that a thin polymer film (*e.g.* 35 μm-thick polydimethylsiloxane (PDMS) film) acts as an effective alternative coupling agent essential for realizing two-chip acoustic tweezers for particle patterning and manipulation. The PDMS film can attach to the SAW device by weak forces. This polymer coupling agent achieves a balance between acoustic coupling efficiency, stability against evaporation at high RF power, and detachability without any damage.

In addition, many reports on two-chip droplet concentration have indicated that Raleigh waves from the SAW device couple into the silicon superstrate as Lamb waves[19] which drive the acoustic forces. A similar wave-type conversion should also apply to two-chip particle manipulation. In this paper, we have used silicon as the superstrate. As the properties of silicon have been extensively studied and documented, we are able to derive the acoustic properties of silicon superstrates in relation to the thickness and frequency of different types of waves and compare them to the separation between particles.

In this work, we describe a two-chip acoustofluidic platform for performing two-dimensional (2D) manipulation of microparticles in a closed microchamber on a disposable silicon superstrate. In the two-chip approach, we found that the standing surface acoustic wave (SSAW) is transmitted into the silicon superstrate *via* the coupling agent to form a standing Lamb wave (SLW). Given that Lamb waves have been used for droplet concentration, it is of interest to verify if Lamb waves can also be used for particle manipulation. The proposed acoustofluidic platform is able to trap suspended microbeads for 2D patterning by controlling the pressure field associated with the SLW on the silicon superstrate. By tuning the excitation frequency using chirped interdigital transducers (IDTs), we were able to trap and move (*i.e.* manipulate) microbeads on the silicon superstrate. After each experiment, the silicon superstrate can be easily detached from the LN substrate, allowing the undamaged SAW device to be reused. Having a removable superstrate is helpful for biological analysis as the superstrate that has been in contact with biological samples can be discarded to prevent cross contamination. In addition to its feature of being reusable, the reported device retains the merits of acoustofluidic particle manipulation of being contactless and label-free, and admissible regardless of the samples' shape, density, polarity and electrical properties.

Materials and methods

Single device fabrication

There were four major steps involved in the fabrication process of the integrated two-chip device: (a) fabrication of a SAW device on an LN substrate, (b) fabrication of a polydimethylsiloxane (PDMS) microchamber, (c) bonding of the PDMS microchamber and PDMS coupling layer onto the silicon chip, and (d) bonding of the silicon superstrate to the SAW device *via* the PDMS coupling layer. Firstly, a layer of AZ 4562 photoresist was spin-coated on a 128° Y cut X-propagation LN wafer, and then patterned using a standard photolithography process (using the photoresist developer AZ 300 MIF). A dual metal layer stack (Cr/Al, 50 Å/5000 Å) was subsequently deposited on the LN wafer using a thermal evaporator, and the IDT electrodes were formed following a lift-off process.

The PDMS microchamber structure (height of 50 μm, diameter of 1000 μm, sidewall thickness of 1000 μm) was fabricated using standard soft-lithography (SU-8 2025 photoresist) and mould-replica techniques. The side walls of the chamber are thinner than the bonding area at the corner of the chip with the aim to reduce acoustic attenuation through the PDMS walls.[20] Next, the Sylgard 184 Silicone Elastomer Curing Agent and Base (Dow Corning) were mixed at a weight ratio of 1 : 10, and then cast on top of a silicon mold and cured at 75 °C for 3 hours. Two holes were punched into the microchannel to create an inlet and an outlet. During the curing process, the same PDMS mixture was spin-coated on an acrylic disk with a speed of 3000 rpm to form a thin polymer layer (approximately 35 μm-thick) as the coupling film. Finally, the PDMS microchamber and the silicon chip were treated in an oxygen plasma cleaner (PDC001, Harrick Plasma) for 1.5 min for bonding and cured overnight. Again, the PDMS thin coupling film was plasma bonded on the other side of the silicon chip.

Two-chip coupling and detachment

The silicon superstrate with the PDMS microchamber can be attached and detached from the SAW device before and after use for a particle manipulation experiment. First, a drop of ethanol (for moving the superstrate to the desired place) was placed on the LN substrate, and covered by the silicon superstrate at the centre of IDT delay lines. The two chips were then baked at 65 °C for 10 min; applying thermal treatment enables van der Waals force adhesion between the two surfaces. Before detaching the silicon superstrate from the LN substrate, adding a drop of ethanol along the edge of the silicon superstrate helps to modulate the adhesion force between the two surfaces. The adhesion is strong enough to hold the two surfaces together during a 2D manipulation experiment, but the silicon superstrate can be peeled off at the end without damaging the SAW device for reuse in the next experiment.

Sample preparation

To characterize the performance of the detachable acoustofluidic platform, polystyrene (PS) microbeads (DaE Scientific, Tianjin, China, density: 1.05 g cm^{-3}) with different diameters was diluted in deionized (DI) water to a concentration of 0.5 mg ml^{-1}. To help prevent particle adhesion to the chamber walls, the non-ionic detergent Tween 20 (Sigma-Aldrich) was used as the surfactant and mixed into DI water to a concentration of about 0.002%–0.003%. The solution of 75% ethanol was injected into the PDMS microchamber to remove the residual microbeads.

Experimental setup

A network analyzer (Agilent Technologies, E5061A, USA) was used to measure the actual resonant frequency and insertion loss for the SAW device. Two digital and vector signal genera-

tors (Agilent Technologies, USA) were used in conjunction with two amplifiers (Mini Circuits ZHL-5W-1, 5–500 MHz) and a 3 A, 24 V DC power supply to power the SAW device. The fabricated acoustofluidic device was mounted on the digital microscope stage (AM73515MT8A, Dino-Lite, Taiwan) to observe the moving track and pattern of the microparticles. Microparticles were infused into the chamber through a 1 ml syringe using a home-made syringe pump. The syringe was cleaned through ethanol injection before each experiment. The acoustofluidic device was positioned on a passive aluminium heat sink to dissipate heat caused by the high input power. The temperature was monitored using an infrared thermometer.

Results and discussion

Design of the two-chip acoustofluidic device

Fig. 1a depicts the proposed two-chip acoustofluidic platform for 2D particle manipulation on a replaceable silicon superstrate, which comprises two interchangeable parts: (1) a detachable silicon superstrate enclosed in a PDMS microchamber and (2) a reusable LN piezoelectric substrate for generating the SAW. The SAW device has two pairs of chirped interdigitated transducers (IDTs), which form a pair of delay lines orthogonal to the other. The delay lines were oriented 45° to the flat of a 128° Y-cut LN wafer. Applying an RF signal to one pair of IDTs sets up a standing SAW (SSAW) along the respective delay line. Driving both pairs of IDTs sets up a 2D standing acoustic wave. Each chirped IDTs (26 pairs of electrodes) has a linearly graded finger pitch (50–75 μm in increments of 1 μm) to allow generation of SAWs over a range of frequencies. The aperture of each set of IDTs was 4.4 cm. To enable 2D particle manipulation on a silicon superstrate, we bonded a PDMS microchamber (diameter: 1 mm, height: 50 μm, sidewall width: 1 mm) on the silicon superstrate (laser cut to a side length of 5.4 mm) by oxygen plasma treatment. As shown in Fig. 1a, the PDMS bonding area at the corners of the chip is notably wider (2 mm) than the side walls of the chamber (1 mm). We reduced the wall thickness in this design with the aim to weaken acoustic attenuation *via* the PDMS walls. The silicon superstrate area is smaller than the aperture of the IDTs to ensure full coverage of the SSAW field. The side with the PDMS microchamber is referred to as the top side of the superstrate. The detailed fabrication and assembling process is described in Fig. S1 (ESI†). An optical image of the fabricated acoustofluidic two-chip device is depicted in Fig. 1c. Considering that LN is well-known to be fragile material, it is worth mentioning the precautionary measures we have adopted for further preventing from breakage for plug-and-play applications. While the proposed adhesion technique for bonding and detaching of the PDMS coupling layer allows safe detachment of the superstrate without damaging the SAW device, we designed a PCB encapsulation frame for the LN SAW device without covering the IDTs and delay line area as shown in Fig. S2.†

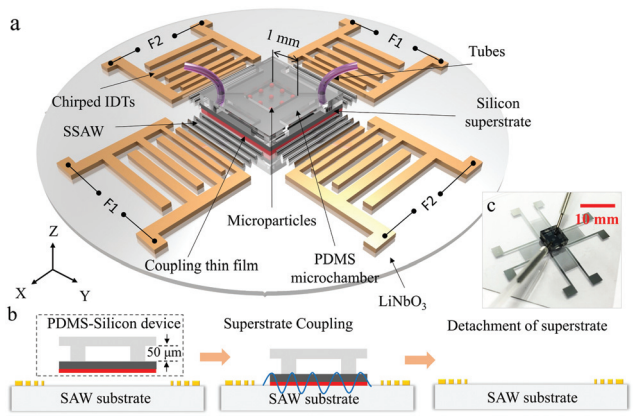

Fig. 1 (a) Perspective view of the two-chip reusable acoustofluidic platform for manipulating microbeads in 2D on a silicon superstrate. (b) Cross-sectional view depicting the sequence of attaching and detaching the silicon superstrate from the LN substrate (SAW device) *via* the PDMS coupling layer on the silicon superstrate without damaging the SAW device. (c) Optical image of the fabricated two-chip acoustofluidic platform shows the PDMS-silicon superstrate coupled with the SAW device.

Coupling method of the acoustic wave

Critical to realizing a two-chip reusable acoustofluidic platform for 2D manipulation is choosing a working coupling agent to interface the SAW device and silicon superstrate. UV epoxy, KY gel and DI water have been used as coupling layers previously.[18] Although these coupling agents offer sufficient acoustic coupling efficiency, they have practical drawbacks. For example, water evaporates rapidly under the RF power levels required for manipulation and thus is unstable over time for experiments. Epoxies and gels provide strong bonding, which makes it difficult to detach the two surfaces without damage. Besides, cleaning up gel coupling agents to reuse the SAW device is impractical. As an alternative, we employed a polymer thin film (*i.e.* PDMS) that is about 35 μm thick as the coupling layer. The mechanical properties of the PDMS coupling layer enable reasonable acoustic coupling. Meanwhile, weak forces over the PDMS surface offer sufficient adhesion to hold the silicon superstrate during operation, and the superstrate can be replaced for new experiments. To form such a coupling layer on the silicon superstrate, PDMS was spin-coated and plasma-bonded on the 'bottom' side of the silicon superstrate (*i.e.* the side facing the SAW device). It is worth pointing out that PDMS being a soft material with a high acoustic attenuation coefficient will absorb part of the acoustic energy from the Rayleigh wave on the LN substrate.[21,22] Therefore, reducing the thickness of the PDMS film can promote higher energy coupling between the SAW device and the silicon superstrate in the microfluidic chamber. However, there are practical limits on thickness variation when fabricating PDMS films, implying that the PDMS film should be sufficiently thick such that its variation is negligible compared to the bulk thickness. In other words, we should obtain a balance between feasibility of fabrication and promoting higher coupling efficiency for realizing the proposed two-chip device.

Fig. 1b illustrates the process of attaching and detaching the silicon superstrate from the SAW device before and after

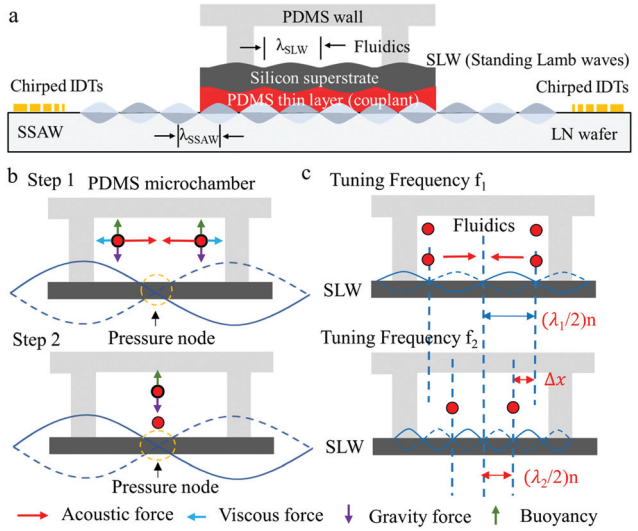

Fig. 2 (a) Cross-sectional view describing the leakage of the SSAW from the LN substrate into the silicon superstrate *via* the coupling layer in the form of standing Lamb waves. (b) External forces acting on microbeads in the process of moving (step 1) and trapping (step 2). (c) Illustration of the principle behind manipulating microbeads by tuning the frequency of the RF signal applied to the chirped IDTs.

use for a particle manipulation experiment. Applying thermal treatment enables van der Waals force adhesion between the two surfaces. The adhesion is strong enough to hold the two surfaces together during a 2D manipulation experiment, but the silicon superstrate can be peeled off at the end without damaging the SAW device for reuse.

As illustrated in Fig. 2a, the generated Rayleigh wave on the SAW device leaks into the PDMS coupling layer from the side edge of the interface, where it is known to couple into the silicon superstrate in the form of a Lamb wave.[23] The resulting vibration on the top surface of the silicon superstrate associated with the Lamb wave transmits acoustic pressure into the fluid encased within the PDMS microchamber.

Analysis of acoustofluidic forces and the working principle

The microchamber was filled with deionized (DI) fluid containing polystyrene (PS) microbeads. In the chamber, the PS microbeads are subjected to four kinds of external forces to maintain an equilibrium state. Along the vertical axis, the balance between buoyancy and gravity results in the state of rest due to the similarity in density between the PS microbeads and DI water, as shown in Fig. 2b. When a standing Lamb wave (SLW) is set up across the silicon superstrate, the microbeads are trapped within the pressure nodes under the influence of the acoustic radiation force (ARF); the ARF is normally much higher than the viscous force (but dependent on the diameter of particles). The primary acoustic force (F_r) exerted on an object in an acoustic field can be expressed as:[24]

$$F_r = -\left(\frac{\pi p_0^2 V \beta_m}{2\lambda}\right) \times \varphi(\beta,\rho) \times \sin(2kx) \quad (1)$$

$$\varphi(\beta,\rho) = \frac{5\rho_c - 2\rho_m}{2\rho_c + \rho_m} - \frac{\beta_c}{\beta_m} \quad (2)$$

$$k = \frac{2\pi}{\lambda} = \frac{\omega}{c_{phase}} \quad (3)$$

where x is the position, p_0, λ, and V are the acoustic pressure, wavelength, and volume of the object respectively, and ρ_c, ρ_m, β_c, and β_m represent the density of the particles, density of the medium, compressibility of the particles, and compressibility of the medium, respectively. Therefore, the amplitude of the acoustic force is related to the frequency of the standing acoustic wave and volume of the object.

Fig. 2c illustrates the principle of manipulation using chirped IDTs. We refer to the stationary pressure node in the centre of the microchamber as the 0th order node, progressing to the 1st, 2nd, 3rd order and onwards as we move outwards from the centre. The location of the nth order pressure node (x_n) is given by,

$$x_n = n\lambda/2 \quad (4)$$

where λ is the wavelength of the Lamb wave. As such, the position of all higher-order ($n > 0$) pressure nodes can be shifted by tuning the signal frequency applied to the chirped IDTs. The node displacement (Δx_n) can be described by:

$$\Delta x_n = n(\lambda_1 - \lambda_2)/2 = n\left(\frac{c}{f_1} - \frac{c}{f_2}\right)/2 \quad (5)$$

where c is the sound wave speed; and f_1 and f_2 are the original and regulated frequencies, respectively. Eqn (5) indicates that the displacement magnitude of the particles is directly proportional to the node order.

Phase velocity of the Lamb wave

As mentioned, the SAW generated on the LN substrate couples into the silicon superstrate and is propagated as a Lamb wave. There are two distinct classes of propagation modes of the Lamb wave: symmetric and antisymmetric, which can be determined using an adaptation of the Rayleigh–Lamb characteristic frequency equations, given by Rose,[25]

Symmetric modes:

$$\frac{\tan\left(\frac{qd}{2}\right)}{\tan\left(\frac{pd}{2}\right)} = -\frac{4k^2pq}{(q^2-k^2)^2}, \quad (6)$$

Antisymmetric modes:

$$\frac{\tan\left(\frac{qd}{2}\right)}{\tan\left(\frac{pd}{2}\right)} = -\frac{(q^2-k^2)^2}{4k^2pq}, \quad (7)$$

$$p^2 = \left(\frac{\omega}{c_L}\right)^2 - k^2, \quad q^2 = \left(\frac{\omega}{c_T}\right)^2 - k^2 \quad (8)$$

where d is the silicon superstrate thickness, ω is the angular frequency, and c_L (9133.8 m s^{-1}) and c_T (5842.9 m s^{-1}) are respectively the longitudinal and transverse velocities.[26] The

manifold solutions of the transcendental equations indicate that the Lamb wave is dispersive such that the phase velocity is a function of the frequency-thickness product. For each given frequency, the phase velocity and modes propagating in the superstrate are dependent on the superstrate thickness. Inversely, for a given silicon superstrate thickness of d = 400 μm, the phase velocities of the lowest order modes can be described in Fig. 3a. In the range of 14–19 MHz excited by the chirped IDTs, more than one asymmetric and three symmetric modes can be excited. However, the phase velocities of the zero-order symmetric (S_0) and antisymmetric (A_0) modes are the closest to that of the propagating Rayleigh wave in the LN substrate (3990 m s^{-1}), and thus these modes are excited preferentially over the higher order modes.

Transmission measurement of the SAW device

The frequency response of the SAW device, shown in Fig. 3b, was measured using a network analyzer. The measured S_{21} verifies the specified wideband excitation frequency range enabled by the chirped IDTs (13.3–19.95 MHz). A slight drop in magnitude within the transmission band was mainly caused by the coupling layer, in which leakage of the Raleigh wave into the superstrate occurred in the form of Lamb waves.

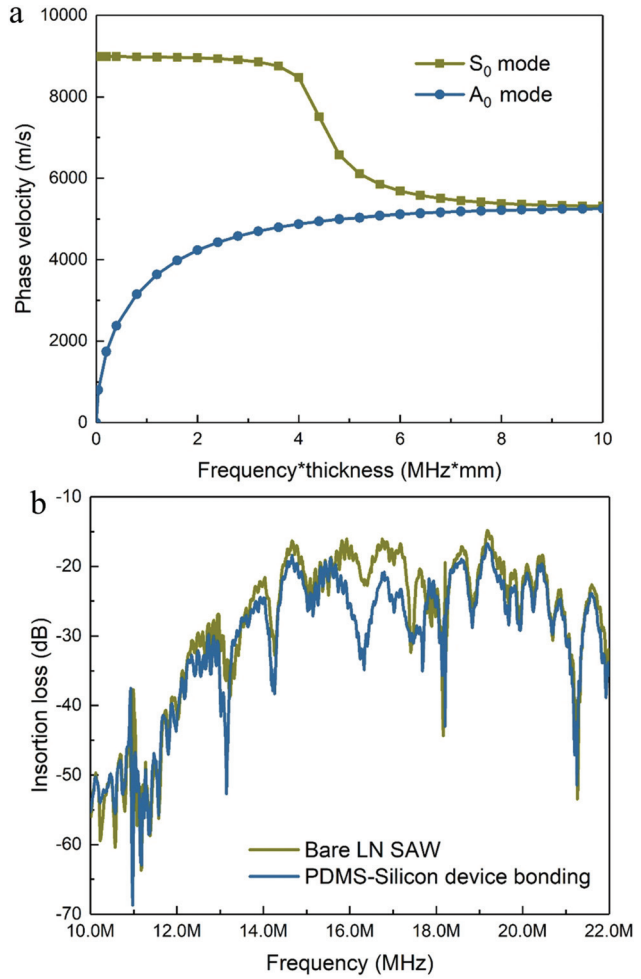

Fig. 3 (a) The dispersion curve of the lowest order mode obtained from the solutions of eqn (6)–(8) for an infinite free silicon chip over the range of the frequency-thickness product 0–10 MHz mm. (b) Comparison of the measured transmission (S_{21}) across a delay line on the SAW device before and after bonding the silicon superstrate on the LN substrate.

Heating effect of the acoustofluidic device

Before the experiment, we also examined heating effects on the SAW device (without the silicon superstrate) and on the silicon superstrate as additional control experiments. As shown in Fig. S3,† the temperature of the SAW device and silicon superstrate increases from ~24.8 °C to ~31.5 °C and 29.5 °C over the 5 minute duration in which the RF signal was applied to two pairs of chirped IDTs (33 dBm). For a given input RF power applied to the SAW device, the amount of heat generated in the superstrate is related to the efficiency of energy coupling by the polymer layer. A higher efficiency of energy coupling by the polymer film will result in a higher proportion of surface acoustic wave energy on the LN SAW substrate leaking into the superstrate as Lamb waves and eventually the thermal energy. As the heat generated is related to the vibration amplitude of the Lamb waves in the superstrate, for the same level of driving RF power, a higher energy coupling efficiency of the polymer film will induce larger heat generation. Upon the application requirements, discrete manipulation periods can be adopted to limit the temperature increase, by providing time between consecutive manipulation periods for heat dissipation.

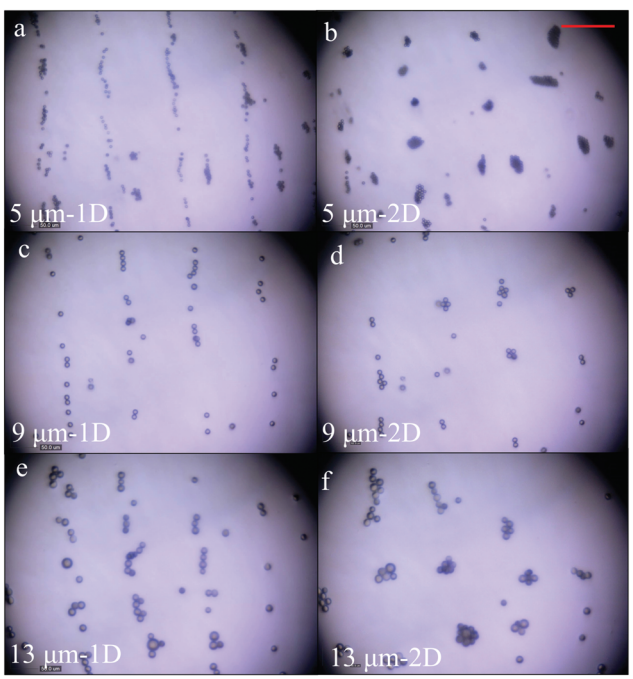

Fig. 4 1D and 2D patterning of PS microbeads with a diameter of (a and b) 5 μm, (c and d) 9 μm and (e and f) 13 μm. The microbeads were initially randomly dispersed, and then the microbeads cluster formed a 1D and 2D array after applying the acoustic wave (19 MHz, 33 dBm). Scale bar (top right): 100 μm.

Demonstration of microparticle patterning

Experiments were conducted to demonstrate the patterning of PS microbeads of three different diameters (5 μm, 9 μm, and 13 μm). The microbeads were injected into the microchamber and the connecting tubing was sealed thereafter. We first patterned the microbeads in one axis (*i.e.* 1D) by generating a SSAW on one axis. As shown in Fig. 4a, c, and e, despite the particle diameter, the microbeads cluster along the parallel pressure node lines. The separation distance between the parallel lines of microbeads corresponded to half the wavelength of the SLW, ranging from 115–135 μm. At 19 MHz, the observed line separation correlates well with the phase velocities of the Lamb wave in (100) silicon (both the symmetric and antisymmetric waves between 5195 m s^{-1} to 5408 m s^{-1}). Next, we patterned the microbeads in 2D by generating SSAWs on both axes (each with the same power of 33 dBm as the 1D case), resulting in the matrix pattern depicted in Fig. 4b, d, and f. Video S1 in the ESI† captures the representative movements of the microbeads under the SSAWs/SLWs.

Quantity analysis of the moving velocity

We then conducted experiments to quantify the travel speed of the microbeads in relation to the input RF power and particle diameter, respectively. In relation to the RF power level, Fig. 5a shows that microbeads with a diameter of 9 μm can reach up to speeds of 79 μm s^{-1} (1D SLW) and 89 μm s^{-1} (2D SLW) at an RF power of 35 dBm. With respect to microbead diameter, the travel speed increases with the size of the microbeads, as shown in Fig. 5b. Increasing the diameter and volume of the PS microbeads increases the ARF, which can be validated by eqn (1). These results suggest that the technique can be applied to cells as their sizes lie in the micron range.

Demonstration of microparticle manipulation

Finally, we have successfully shifted the position of microbeads (*i.e.* particle manipulation) on the disposable silicon superstrate by tuning the RF signals applied to the SAW device. Fig. 6a shows the movement of the microbeads as the frequency of the RF signals is tuned along one axis at a time.

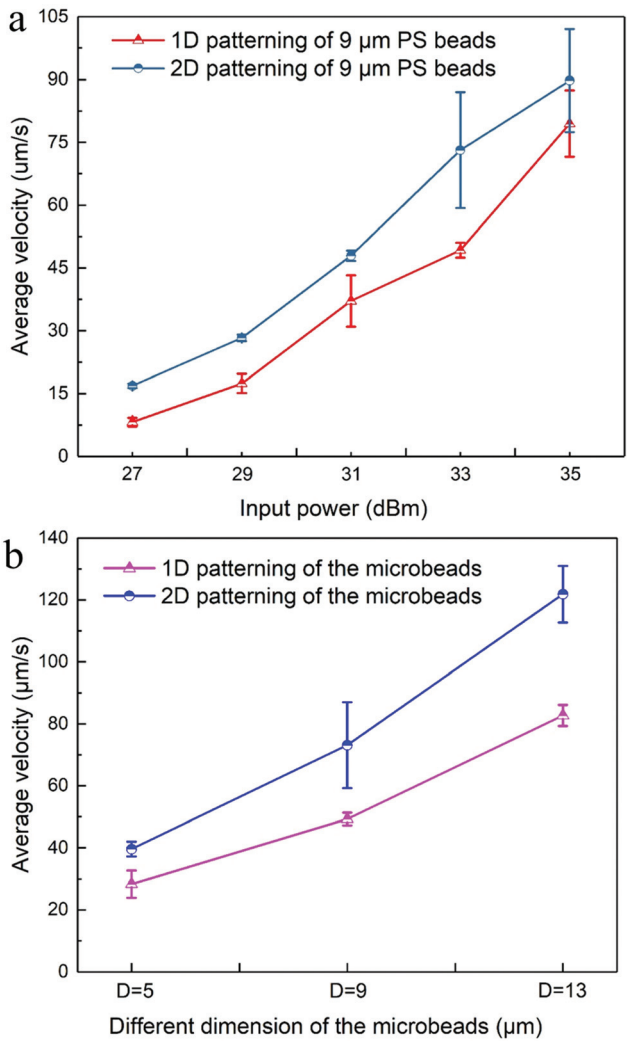

Fig. 5 Velocity of microparticles in the microfluidic chamber on the silicon superstrate as a function of the (a) input RF power level and (b) diameters of the microbeads. The input power used in (b) is 33 dBm. The excitation frequency for both (a) and (b) was 19 MHz. Error bars are the standard deviations. $N \geq 3$.

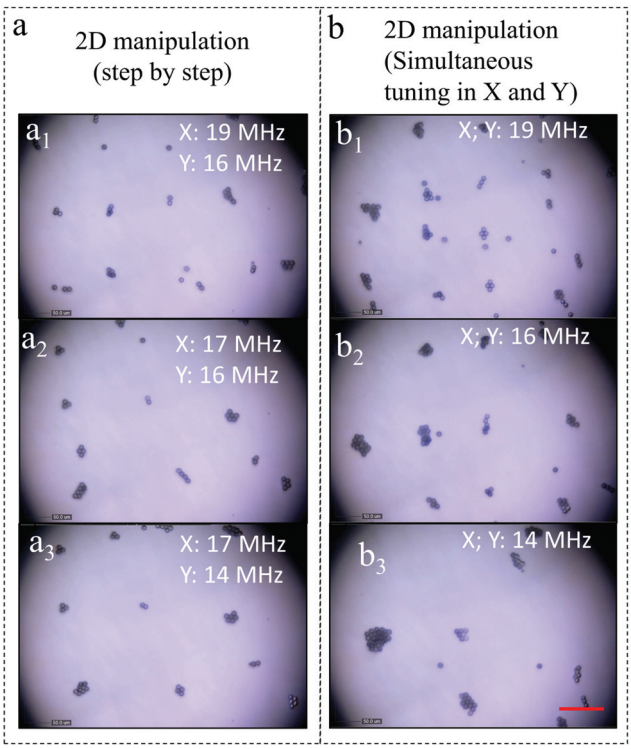

Fig. 6 2D manipulation of PS microbeads with a diameter of 9 μm. (a) Manipulation of microbeads independently along the *x*-axis (by changing the frequency along the *x*-axis from 19 MHz to 17 MHz) followed by the *y*-axis (by changing the frequency along the *y*-axis from 16 MHz to 14 MHz). (b) 2D manipulation from simultaneously shifting the frequency in both axes from 19 MHz to 14 MHz. Scale bar (bottom right): 100 μm.

From a_1 to a_2, decreasing the frequency along the *x*-axis increased the separation along the *x*-axis. Then from a_2 to a_3, decreasing the frequency along the *y*-axis increased the separation along the *y*-axis while separation along the *x*-axis remained unchanged. Fig. 6b shows the movement of the microbeads when the RF signal frequencies on both axes are tuned simultaneously. In this case, the microbeads reorganize to the nearest new nodes (corresponding to the new frequency) in the form of a 2D matrix. Video S2 in the ESI† captures the process of 2D manipulation. Notably, the microbeads do not necessarily move in the same direction with the shift of frequency but move to the nearest node. This is due to the symmetry of the microchamber relative to the delay line. In our case, the centre of the microchamber lies on the 0^{th} order node. As discussed in S4,† offsetting the centre of the microchamber will help skew the particles to move in the same direction.

Conclusion

In this work, we have demonstrated a two-chip acoustofluidic platform for 2D particle manipulation on a replaceable silicon superstrate. The device allows us to trap suspended microbeads for 2D patterning or transport by controlling the pressure field associated with the SLW on the silicon superstrate. Using a thin polymer coupling layer, we are able to reliably fix the silicon superstrate on the SAW device to enable acoustic transmission from the SAW device to the silicon superstrate during manipulation experiments. The silicon superstrate can be easily detached from the SAW device after the experiments, allowing the undamaged SAW device to be reused. In addition to the advantage of reusability, the reported method retains advantages of acoustofluidic particle manipulation of being contactless and label-free, and admissible regardless of the samples' shape, density, polarity and electrical properties.

Conflicts of interest

There are no conflicts to declare.

Acknowledgements

The work described in this paper was supported by a grant from the Research Grants Council of Hong Kong under project number CityU 11218118.

References

1 J. Shi, H. Huang, Z. Stratton, Y. Huang and T. J. Huang, *Lab Chip*, 2009, **9**, 3354–3359.
2 M. Yu, S. Stott, M. Toner, S. Maheswaran and D. A. J. Haber, *Cell Biol.*, 2011, **192**, 373–382.
3 Z. Ma, D. J. Collins, J. Guo and Y. Ai, *Anal. Chem.*, 2016, **88**, 11844–11851.
4 B. N. Johnson and R. Mutharasan, *Analyst*, 2017, **142**, 123–131.
5 A. Dalili, E. Samiei and M. Hoorfar, *Analyst*, 2019, **144**, 87–113.
6 Y. Xie, Z. Mao, H. Bachman, P. Li, P. Zhang, L. Ren, M. Wu and T. J. Huang, *J. Biomech. Eng.*, 2020, **142**, 031005.
7 P. Zhang, H. Bachman, A. Ozcelik and T. J. Huang, *Annu. Rev. Anal. Chem.*, 2020, **13**, 17–43.
8 S. Zhao, M. Wu, S. Yang, Y. Wu, Y. Gu, C. Chen, J. Ye, Z. Xie, Z. Tian, H. Bachman, P. H. Huang, J. Xia, S. P. Zhang, H. Zhang and T. J. Huang, *Lab Chip*, 2020, **20**, 1298–1308.
9 Z. Tian, S. Yang, P.-H. Huang, Z. Wang, P. Zhang, Y. Gu, H. Bachman, C. Chen, M. Wu, Y. Xie and T. J. Huang, *Sci. Adv.*, 2019, **5**, eaau6062.
10 X. Ding, P. Li, S.-C. S. Lin, Z. S. Stratton, N. Nama, F. Guo, D. Slotcavage, X. Mao, J. Shi, F. Costanzo and T. J. Huang, *Lab Chip*, 2013, **13**, 3626–3649.
11 A. Ozcelik, J. Rufo, F. Guo, Y. Gu, P. Li, J. Lata and T. J. Huang, *Nat. Methods*, 2018, **15**, 1021–1028.
12 W. Connacher, N. Zhang, A. Huang, J. Mei, S. Zhang, T. Gopesh and J. Friend, *Lab Chip*, 2018, **18**, 1952–1996.
13 S. P. Zhang, J. Lata, C. Chen, J. Mai, F. Guo, Z. Tian, L. Ren, Z. Mao, P. H. Huang, P. Li, S. Yang and T. J. Huang, *Nat. Commun.*, 2018, **9**, 2928.
14 D. J. Collins, B. Morahan, J. G. Bustos, C. Doerig, M. Plebanski and A. Neild, *Nat. Commun.*, 2015, **6**, 8686.
15 M. Wu, P. H. Huang, R. Zhang, Z. Mao, C. Chen, G. Kemeny, P. Li, A. V. Lee, R. Gyanchandani, A. J. Armstrong, M. Dao, S. Suresh and T. J. Huang, *Small*, 2018, **14**, 1801131.
16 X. Ding, S. C. S. Lin, B. Kiraly, H. Yue, S. Li, I. K. Chiang, J. Shi, S. J. Benkovic and T. J. Huang, *Proc. Natl. Acad. Sci. U. S. A.*, 2012, **109**, 11105–11109.
17 G. Destgeer and H. J. Sung, *Lab Chip*, 2015, **15**, 2722–2738.
18 F. Guo, Y. Xie, S. Li, J. Lata, L. Ren, Z. Mao, B. Ren, M. Wu, A. Ozcelik and T. J. Huang, *Lab Chip*, 2015, **15**, 4517–4523.
19 R. P. Hodgson, M. Tan, L. Yeo and J. Friend, *Appl. Phys. Lett.*, 2009, **94**, 024102.
20 I. Bernard, A. A. Doinikov, P. Marmottant, D. Rabaud, C. Poulain and P. Thibault, *Lab Chip*, 2017, **17**, 2470–2480.
21 S. M. Langelier, L. Y. Yeo and J. Friend, *Lab Chip*, 2012, **12**, 2970–2976.
22 M. C. Jo and R. Guldiken, *Microelectron. Eng.*, 2014, **113**, 98–104.
23 C. Witte, J. Reboud, R. Wilson, J. M. Cooper and S. L. Neale, *Lab Chip*, 2014, **14**, 4277–4283.
24 J. Shi, D. Ahmed, X. Mao, S. C. Lin, A. Lawit and T. J. Huang, *Lab Chip*, 2009, **9**, 2890–2895.
25 J. L. Rose, *Ultrasonic Waves in Solid Media*, Cambridge University Press, 2004.
26 H.-J. Kim, S. Kwon and Y. H. Kim, 2013 Joint UFFC, EFTF and PFM Symposium, 2013, DOI: 10.1109/ULTSYM.2013.0416.